

Two-domain model of light-induced structural changes in hydrogenated amorphous silicon

Jonathan Baugh and Daxing Han*

Department of Physics and Astronomy, University of North Carolina, Chapel Hill, North Carolina 27599-3255

(Received 28 September 2001; revised 17 May 2002; published 23 September 2002)

A phenomenological model is proposed to explain an observed light-induced volume expansion in hydrogenated amorphous silicon (*a*-Si:H). Reported evidence strongly suggests that device-quality *a*-Si:H is heterogeneous on the nanometer scale. A heterogeneous network is considered here as a two-domain matrix composed of high- and low-density amorphous domains. The boundaries linking domains are considered to be structurally unstable during illumination due to the effect of light-induced hydrogen migration on the initial distribution of lattice strain. The observed volume expansion can be explained by a decrease in the volume fraction of the high-density domains due to the slight propagation of domain boundaries during illumination.

DOI: 10.1103/PhysRevB.66.115203

PACS number(s): 78.66.Jg

I. INTRODUCTION

The light-induced electronic metastability in hydrogenated amorphous silicon¹ (*a*-Si:H) grown by chemical vapor deposition is still a major obstacle to its application in solar cells despite significant improvements in material quality, such as the achievement defect state densities² as low as $\leq 10^{16} \text{ cm}^{-3}$ and microvoid contents as low as $< 0.1\%$.³ Recently, it was reported that this effect, the so-called Staebler-Wronski effect (SWE), is accompanied by a metastable volume expansion of the order of 10^{-5} – 10^{-6} that follows kinetics similar to those of the SWE,^{4–6} and anneals out at similar temperatures. Furthermore, neither the expansion nor the photoinduced defects are detected in dehydrogenated and microcrystalline (μc -Si:H) samples. The global structural changes implied by the volume expansion were not theoretically anticipated in *a*-Si:H, and there is no existing model to explain them. Here, we construct a phenomenological model of structural changes that could explain the observed volume expansion. The proposed structural changes may also play a role in the SWE, although a detailed investigation in that direction is beyond the scope of this work.

An overview of the heterogeneity of the *a*-Si:H network, including the hydrogen distribution, is given in Sec. II. In Sec. III, the details of the phenomenological model are given. The paper is summarized in Sec. IV.

II. HETEROGENEITY OF *a*-Si:H AT NANOSCALE

A. Overview

There is much evidence to suggest that device-quality *a*-Si:H film is inhomogeneous at the nanometer scale.^{7–10} Film growth by chemical vapor deposition (CVD) begins with nucleation, which can be seen in scanning tunneling microscope images of the first few nanometers of growth of *a*-Si:H on Si surfaces.¹¹ These images reveal nanometer-scale islands that produce surface roughness (rms) of ~ 0.3 – 0.5 nm. Ideal CVD conditions should lead to the disappearance of this nanostructure after the first few layers.¹² However, recent results of fluctuation transmission electron microscopy (TEM) applied to bulk device-quality *a*-Si:H (~ 20 nm thickness) suggest a high density ($\sim 20\%$) of ~ 1 – 3 nm sized domains dubbed “paracrystallites” that are topo-

graphically crystalline, but highly strained, and embedded in an amorphous matrix.¹³ Furthermore, standard high-resolution TEM of high-quality ~ 50 -nm-thick film has led to observations of unexpected nanoscale features in both standard and H_2 -dilution *a*-Si:H samples that indicate ordered regions.¹⁴ Thus it appears that growth processes other than initial nucleation lead to nanoscale fluctuations in configurational order (and thus particle density), which persist throughout film growth. One possibility is that the large affinity of Si for forming a topologically crystalline phase causes continual “nucleation” of such paracrystallites on the growth surface. The network then tends to minimize its strain energy by accumulating strained bonds in the interfacial regions between the paracrystallite edge and the amorphous matrix, forming domain boundaries similar in nature to grain boundaries in microcrystalline material, though probably less distinct. H_2 dilution of the reaction gas is known to increase the volume fraction of ordered regions^{14,15} and narrow the electronic band tail of *a*-Si:H.^{16,17} H_2 dilution may reduce the paracrystallite strain by eliminating many of the weak bonds. A large reduction in this strain could promote the growth of microcrystallites from a fraction of the precursor paracrystallites as the film grows thicker. Hence, high H_2 dilution yields a microcrystalline material (μc -Si:H) characterized by conical crystallites oriented in the growth direction.¹⁴ We note that *a*-Si:H-based solar cells fabricated with the intrinsic layer deposited with optimal H_2 dilution are typically the most stable against SWE-type degradation.⁵

We will use the term “domain” to emphasize that all regions in *a*-Si:H are effectively amorphous (e.g., as far as x-ray and Raman spectroscopy detection), but may exhibit different local structural order and/or topologies. The more ordered domain type—suggested by Gibson *et al.* (Ref. 13) to be paracrystalline—is identified as having higher average particle density than the less ordered domain. This is indicated schematically in Fig. 1(a). In this two-domain (TD) picture, film to film differences in mass density would mainly reflect differences in the relative volume fractions of the two domain types.

There is evidence that both the electronic and structural metastabilities of *a*-Si:H involve hydrogen (H).^{12,18–20} How is the incorporation of H affected by network heterogeneity? It is well known that H is inhomogeneously distributed in

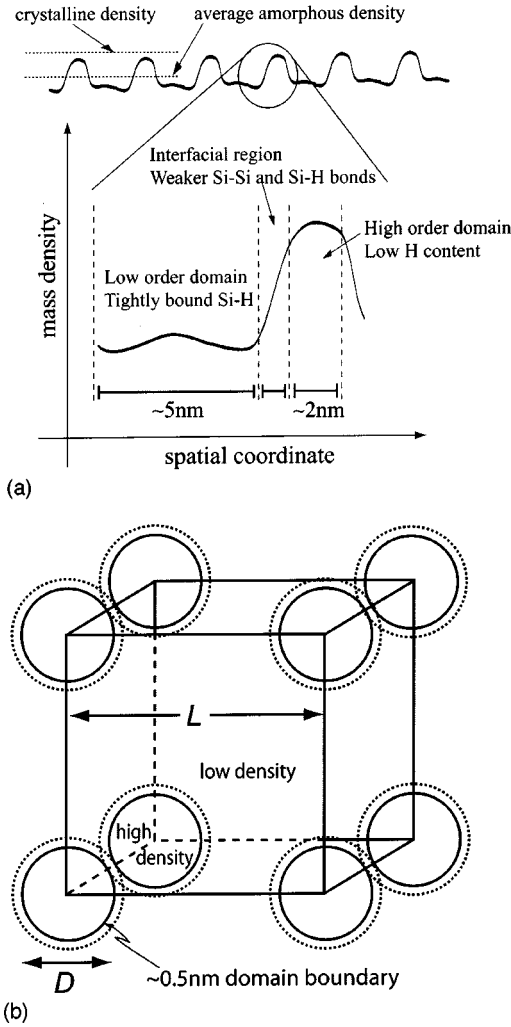


FIG. 1. (a) Schematic illustration of a spatially modulated mass density profile (in one dimension) as a model of a -Si:H. The dense domain size of ~ 2 nm is based on the fluctuation TEM results reported in Ref. 10. (b) Schematic of an idealized “crystal lattice” of high-density domains embedded in a low-density matrix upon which the calculations in Sec. III A are based. A 10% volume fraction of high-density domains could be represented by a “unit-cell” dimension of $L \approx 3.5$ nm and domain diameter $D \approx 2$ nm. Note that there is one dense domain per unit cell. A domain boundary of approximately one atomic layer is indicated in the figure.

a -Si:H. All proton (^1H) nuclear-magnetic-resonance (NMR) studies to date have confirmed that there exist both clustered and isolated phases of Si bonded H, in similar amounts.⁷ Moreover, the clustered H is more weakly bound than the isolated H.²¹ Proton NMR also indicates that there exist volume fractions from ~ 20 – 70 % that contain little or no isolated bonded H.^{7,9} Small-angle neutron scattering (SANS) has recently detected heterogeneity of the H distribution in device-quality plasma-enhanced chemical vapor deposition (PECVD) and hot-wire chemical vapor deposition (HWCVD) films;⁸ similar SANS data were previously interpreted to indicate either a shell-like (two-dimensional) or a filamentary (one-dimensional) H distribution.²² We suggest that the hydrogen distribution follows the spatial fluctuations

of the a -Si network. As mentioned above, lattice strain is built up in the interfacial shells surrounding the ordered domains during the film growth. Weak bonds serve as relatively abundant low-energy sites for H,²³ and significant strain can be relieved by hydrogenation of the interfacial regions. Hence, the majority of the hydrogen incorporated beyond the concentration necessary for passivation of dangling bonds (~ 2 orders of magnitude lower than typical H concentrations of device-quality film) would be absorbed by the interfacial regions in this TD picture. This would produce a filamentary or a shell-like H distribution consistent with the SANS data. The ordered regions would contain very little H, and the majority of the “boundary H” would be in the clustered phase according to the ^1H -NMR spectra.

B. Estimate of density fluctuations

An upper estimate of the magnitude of nanometer-scale density fluctuations may be obtained by comparing films grown by PECVD and HWCVD, respectively. These two types of device-quality films exhibit differences in overall microstructure that have been well studied. For example, HWCVD films²⁴ typically have much higher surface roughness,⁵ lower H content, and are more dense²⁵ compared to PECVD films, and have likewise been reported to exhibit differences in the metastable behavior of electronic properties.⁵ Mass densities for both types of films have been measured by optical methods²⁵ and the flotation method.^{3,26} Low void content ($<0.1\%$) PECVD a -Si:H has a density ~ 2.24 g cm $^{-3}$, whereas HWCVD material is as dense as 2.29 g cm $^{-3}$, with similarly low void content. The H-poor volume fractions of each detected by ^1H NMR are about 10–30 % in PECVD and 70–80 % in HWCVD.⁹ The average mass density of a TD network is (neglecting the boundary regions)

$$\rho \approx \rho_{\text{high}} \nu_{\text{high}} + \rho_{\text{low}} \nu_{\text{low}}, \quad (1)$$

where ρ_{high} , ρ_{low} and ν_{high} , ν_{low} are the densities and volume fractions of high- and low-density domains, respectively. Assuming that only the domain volume fractions vary from film to film, the values $\rho_{\text{high}} \approx 2.31$ g cm $^{-3}$ and $\rho_{\text{low}} \approx 2.23$ g cm $^{-3}$ are estimated from Eq. (1) and from the measured mass densities of the HWCVD and PECVD films. These values give an upper bound on the average density fluctuation of $(\rho_{\text{high}} - \rho_{\text{low}})/\langle \rho \rangle \sim 3\%$. However, because they occur at nanoscale, even such large fluctuations are nearly impossible to detect experimentally, and we stress that device-quality films are quite *uniform* at the length scales commonly probed, e.g., by standard TEM.

C. Metastable site density

The most simple and straightforward physical explanation of the volume expansion is that there exists a density of structurally metastable atomic-scale sites, two-level systems in the simplest case, with annealing energy barriers E_{ann} . The metastable configurations are excited by some process related to illumination and are on average less dense (increased volume) compared to the initial configurations; the

low densities of the metastable states are correlated with their increased structural disorder. Once the light is turned off, all occupied excited states for which the annealing energy barrier $E_{\text{ann}} \gg k_B T$ will be frozen in. The local [left side of Eq. (2)] and global (right side) changes can be related by

$$N_{\text{meta}} \frac{\langle \Delta N_{\text{Si}} \rangle}{N_{\text{Si}}} \sim N_{\text{Si}} \left\| \frac{\Delta V}{V} \right\|, \quad (2)$$

where N_{Si} is the average density of Si atoms ($5 \times 10^{22} \text{ cm}^{-3}$), $\langle \Delta N_{\text{Si}} \rangle$ is the average local density change at a metastable site, N_{meta} is the density of metastable sites and $\|\Delta V/V\| \sim 10^{-5} - 10^{-6}$ is the volume expansion at saturation.^{4,5} The upper limit of $\langle \Delta N_{\text{Si}} \rangle / N_{\text{Si}}$ is of the order of the density fluctuation estimated in Sec. IIB, i.e., $\sim 3\%$. Hence, $N_{\text{meta}} \geq 1 \times (10^{18} - 10^{19}) \text{ cm}^{-3}$, which is about 1–3 orders of magnitude larger than the typical light-induced defect density associated with the SWE. In fact, Stratakis *et al.* (Ref. 6), using a scanning probe microscopy technique, measured a larger volume expansion $\|\Delta V/V\| \sim 10^{-4}$ that corresponds to $\sim 10^{20} \text{ cm}^{-3}$ metastable sites. We conclude, as do Refs. 4 and 6, that the volume change is not caused by the SWE defect creation, but appears to occur in conjunction with it or as a precursor (or possibly, is unrelated). In the following section we propose that the nanoscale heterogeneity of *a*-Si:H could give rise to a light-induced structural metastability consistent with the density of metastable sites obtained in this section.

III. MODEL

A. Domain boundaries and their motion

Figure 1(a) is a schematic illustration of a spatially modulated mass density profile (in one dimension) as a model of *a*-Si:H. The dense domain size of $\sim 2 \text{ nm}$ is based on fluctuation TEM results.¹⁰ The interfacial region is also indicated in the figure, as well as the dominant type of hydrogenation in the three regions. Figure 1(b) is a three-dimensional schematic of an idealized “crystal lattice” of high-density domains embedded in a low-density matrix. A 10% volume fraction of high-density domains—suggested as typical for PECVD films (see Sec. IIB)—could be represented by a “unit-cell” dimension $L \approx 3.5 \text{ nm}$ and domain diameter $D \approx 2 \text{ nm}$. A domain boundary roughly one atomic layer thick, 4 \AA , would yield a volume fraction of boundaries $\sim 15\%$ for these values of L and D . Explicitly, the total cell volume is $L^3 = 42 \text{ nm}^3$, the volume of the dense domain is $V_{\text{high}} \approx D^3/2 = 4 \text{ nm}^3$, and the domain boundary volume is $V_B \approx 3D^2\delta + 6D\delta^2 = 7 \text{ nm}^3$ for boundary thickness $\delta = 0.4 \text{ nm}$. Hence, the unit-cell volume of the low-density matrix is in this case $L^3 - V_{\text{high}} - V_B \approx 31 \text{ nm}^3$. Let us assume for the moment that the boundary regions are unstable under illumination and tend to encroach on the high-density domains, effectively decreasing the volume fraction of high-density domains. The following shows that a very slight encroachment will lead to the observed magnitude of the volume expansion. The global volume change can be expressed as

$$\frac{\Delta V}{V} \approx \left(\frac{\rho_{\text{high}} - \rho_{\text{low}}}{\langle \rho \rangle} \right) \left(\frac{V_{\text{high}} - V'_{\text{high}}}{L^3} \right), \quad (3)$$

where V'_{high} is the average volume of the dense domains after illumination, and we have assumed that the density of the encroaching boundary region is equal to ρ_{low} . Given $\Delta V/V \sim 10^{-5}$ from experiment and an estimate of $(\rho_{\text{high}} - \rho_{\text{low}})/\langle \rho \rangle \sim 1\%$ consistent with Sec. IIB, we find that $V_{\text{high}} - V'_{\text{high}} \approx 0.04 \text{ nm}^3$, or a 1% decrease in V_{high} . This corresponds to an *average* displacement of the domain boundary interface of $\Delta x \approx \Delta V_{\text{high}}/3D^2 = 0.003 \text{ nm}$, an exceedingly small motion. The density of metastable sites associated with this domain boundary motion is $N_{\text{meta}} \approx (\Delta V_{\text{high}}/L^3)N_{\text{Si}} = 5 \times 10^{19} \text{ cm}^{-3}$, consistent with the quantity estimated in Sec. IIC. Hence, a small fraction ($\leq 1\%$) of these metastable sites could generate the typically observed density of Staebler-Wronski defects ($\sim 10^{17} \text{ cm}^{-3}$). We note that the number of metastable sites (e.g., net increased-volume sites after light soaking) per dense domain is roughly only $N_{\text{meta}}L^3 \approx 2$ per 10^{-5} volume expansion.

B. Phenomenological arguments

Why would we suppose that the aforementioned boundaries would be unstable under illumination? There are two main reasons. First is the enhancement of phonon creation and absorption in the domain boundary regions. We have supposed that the domain boundaries contain the majority of highly strained bonds in the material, and are therefore where the majority of the electronic band tail states are located. The fraction of all bonds that are weak bonds in typical device-quality *a*-Si:H varies from 0.1% to 1% depending on the values one uses for the density of states at the conduction band edge (see, for example, Ref. 12). Since the volume fraction of domain boundaries is $\sim 10\%$, then roughly 1–10% of the boundary-associated bonds are weak bonds in the TD model. Electronic carriers excited by illumination tend to thermalize into the band tail states prior to recombination,^{12,27} hence the nonradiative recombinations that produce phonons will mostly take place near the domain boundaries. Furthermore, the phonons are more likely to be absorbed by the lattice where the electrons are most localized,²⁸ again the domain boundaries. The second factor is the role of hydrogen. We have discussed how the heterogeneity of the H distribution in *a*-Si:H appears to follow the backbone heterogeneity of the *a*-Si network. When excessive free energy is available in the form of phonons due to non-radiative carrier recombination ($\sim 1.4 \text{ eV}$ per event), Si-H bonds are susceptible to being broken.¹² This is particularly true for paired configurations like Si-H H-Si, in which weak Si-Si bonds can reform upon the removal of both H's, lowering the effective energy barrier to H emission.²³ Since the bulk of this weakly bound, clustered hydrogen is thought to be associated with domain boundaries in the TD picture, illumination will cause H to migrate out of the boundaries—into the amorphous matrix as well as into the dense, ordered domains. It has been suggested²³ that the pairwise insertion of H into a strained weak bond can transport the weak bond to neighboring atoms, whereas the reverse reaction can also

take place. This provides a mechanism by which the distribution of lattice strain can be altered by the motion of hydrogen.²³ This mechanism was proposed to explain a marked decrease in the crystalline phase in H-plasma treated μ c-Si:H that was found to require the presence of grain boundaries (hence, their motion).²⁹ The authors of that work propose that the motion of the grain boundaries in their experiment is driven by minimization of lattice strain energy. We suggest the possibility that light-induced H migration causes similar motion, albeit slight, of the domain boundaries in a TD α -Si:H network. In this case, the driving force for the structural changes is the excess free energy under illumination due to carrier recombination. The localized, non-thermal-equilibrium deposition of phonon energy tends to cause the out diffusion of hydrogen, and therefore strain, from the domain boundaries, leading the domain boundaries to shift toward the dense domains. This process is identified with a decrease in the volume fraction of dense domains and therefore with the global volume expansion. Both the total configurational disorder and the disorder of the strain distribution are increased in this process.

The redistribution of strain (e.g., boundary motion) described above is not a relaxation process, but rather increases the compressive stress of the film^{4,5} and raises the total lattice strain energy. On the other hand, the total Si-Si bonding energy (e.g., configurational energy) of the material should only fluctuate about a nearly constant value, going through maxima and minima as the boundary motion occurs. The strain energy, increasing more sharply with boundary motion, adds to this so that on average the total energy increases as the motion proceeds. In this way the local minima of total energy, which occur as the boundaries move, are raised in energy relative to the initial state, and are thus metastable.

This explains the observation that the volume expansion reverses upon annealing.^{4,6} The fact that the annealing temperature is only 200 °C (Ref. 4) suggests that thermal activation of hydrogen motion¹² is sufficient to surmount the energy barriers back to lower-energy structural states.

IV. SUMMARY

We have proposed a phenomenological model that yields a straightforward connection between the heterogeneity of α -Si:H, its hydrogen distribution, and its light-induced metastable structural changes. The main feature are: (1) the majority of strained, weak Si-Si bonds are associated with domain boundaries in a two-domain network; (2) light-induced phonon creation and absorption is therefore enhanced in the domain boundaries; (3) the clustered H found in α -Si:H is also a characteristic of the domain boundaries; (4) light-induced migration of H transports the strain associated with the domain boundaries into the dense domains, causing the volume expansion; and (5) the changes are metastable due to the increase in total lattice strain energy.

Comparing measurements of the volume expansion for pure α -Si:H and mixed-phase α -Si:H would be worthwhile, since recent observations³⁰ suggest that light-induced structural changes could be significantly larger in some of the latter films. Also, detailed theoretical investigation via molecular-dynamics simulations could provide a rigorous test of the feasibility of the model.

ACKNOWLEDGMENTS

This work was supported by the NREL through Contract Nos. XAK-8-17619-11 and RDJ-1-30630-09 under the Thin Film Partnership.

*Author to whom correspondence should be addressed. Email address: daxing@physics.unc.edu

¹D. L. Staebler and C. R. Wronski, Appl. Phys. Lett. **31**, 292 (1977).

²Y. Lubianiker *et al.*, J. Non-Cryst. Solids **266**, 253 (2000).

³D. L. Williamson, in *Amorphous Silicon Technology—1995*, edited by M. Hask, E. A. Schiff, M. Powell, A. Matsuda, and A. Madan, Mater. Res. Soc. Symp. Proc. No. 377 (Materials Research Society, Pittsburgh, 1995), p. 251.

⁴T. Gotoh *et al.*, Appl. Phys. Lett. **72**, 2978 (1998).

⁵D. X. Han, J. Baugh, G. Z. Yue, and Q. Wang, Phys. Rev. B **62**, 7169 (2000).

⁶E. Stratakis, E. Spanakis, H. Fritzche, and P. Tzanetakis, J. Non-Cryst. Solids **266–269**, 506 (2000).

⁷J. A. Reimer, R. W. Vaughan, and J. C. Knights, Phys. Rev. B **24**, 3360 (1981).

⁸D. L. Williamson *et al.*, in *Amorphous and Heterogeneous Silicon Thin Films—2000*, edited by R. W. Collins, H. M. Branz, S. Guha, H. Okamoto, and M. Stutzmann, Mater. Res. Soc. Symp. Proc. No. 609 (Materials Research Society, Pittsburgh, 2001), p. A16.2.

⁹Y. Wu *et al.*, Phys. Rev. Lett. **77**, 2049 (1996).

¹⁰M. M. J. Treacy, J. M. Gibson, and P. J. Keblinski, J. Non-Cryst. Solids **231**, 99 (1998).

¹¹D. M. Tanenbaum, A. Laracuente, and A. C. Gallagher, in *Amorphous Silicon Technology—1995*, edited by M. Hask, E. A. Schiff, M. Powell, A. Matsuda, and A. Madan, Mater. Res. Soc. Symp. Proc. No. 377 (Materials Research Society, Pittsburgh, 1995), p. 143.

¹²R. A. Street, *Hydrogenated Amorphous Silicon* (Cambridge University Press, Cambridge, England, 1991).

¹³J. M. Gibson, M. M. J. Treacy, P. M. Voyles, H. C. Jin, and J. R. Abelson, Appl. Phys. Lett. **73**, 3093 (1998).

¹⁴D. V. Tsu, B. S. Chao, S. R. Ovshinsky, S. Guha, and J. Yang, Appl. Phys. Lett. **71**, 1317 (1997).

¹⁵S. Guha *et al.*, Appl. Phys. Lett. **74**, 1860 (1999).

¹⁶G. Z. Yue *et al.*, Appl. Phys. Lett. **77**, 3185 (2000).

¹⁷D. X. Han, K. Wang, and L. Y. Yang, J. Appl. Phys. **80**, 2475 (1996).

¹⁸R. Weil, A. Busso, and W. Beyer, Appl. Phys. Lett. **53**, 2477 (1988).

¹⁹W. B. Jackson, Philos. Mag. Lett. **59**, 103 (1989).

²⁰S. R. Sheng, E. Sacher, and A. Yelon, J. Non-Cryst. Solids **282**, 165 (2001).

²¹W. E. Carlos and P. C. Taylor, Phys. Rev. B **26**, 3605 (1982).

²²A. Menelle, J. Non-Cryst. Solids **97–98**, 337 (1987).

²³N. H. Nickel and W. B. Jackson, Phys. Rev. B **51**, 4872 (1995).

- ²⁴A. H. Mahan, B. P. Nelson, S. Salamon, and R. S. Crandall, J. Non-Cryst. Solids **137**, 657 (1991).
- ²⁵Z. Remes, M. Vanecek, A. H. Mahan, and R. S. Crandall, Phys. Rev. B **56**, 12 710 (1997).
- ²⁶J. Baugh, D. X. Han, A. Kleinhammes, and Y. Wu, Appl. Phys. Lett. **78**, 466 (2001).
- ²⁷M. Stutzmann, W. B. Jackson, and C. C. Tsai, Phys. Rev. B **32**, 23 (1985).
- ²⁸J. Li and D. A. Drabold, Phys. Rev. Lett. **85**, 2785 (2000).
- ²⁹I. Kaiser, N. H. Nickel, W. Fuhs, and W. Pilz, Phys. Rev. B **58**, R1718 (1998).
- ³⁰K. Lord, B. Yan, J. Yang, and S. Guha, Appl. Phys. Lett. **79**, 3800 (2001).